... PREDICTS CORTICAL STRAINS UNDER ACETABULAR LOADING

MRL

*Andrew E. Anderson; #Christopher L. Peters; *Benjamin D. Tuttle; *# Jeffrey A. Weiss

*Departments of *Bioengineering & #Orthopaedics, University of Utah, Salt Lake City, Utah*

THE UNIVERSITY OF UTAH

INTRODUCTION

An improved understanding of the stress distribution in and around the hip joint may provide important information regarding the relationship between altered pelvic and acetabular geometry and development of hip osteoarthritis, as well as point to improved diagnostic methods and analysis of surgical treatment. It is very difficult to accurately assess how changes in pelvic geometry affect the stress and strain distribution of the joint in an experimental setting. The finite element (FE) method provides an alternative approach for study of hip joint mechanics. The objectives of this study were to 1) develop and validate a FE model of the pelvis using subject-specific measurements of bone geometry as well as location-dependent cortical thickness and trabecular bone elastic modulus, and 2) assess the sensitivity of the subject-specific FE model to changes in measured and assumed inputs.

METHODS

A combined experimental and computational protocol was used to develop and validate a subject-specific three-dimensional FE model of a 68 y/o female pelvis.

Experimental Protocol -

- Sacroiliac joint and all soft tissue, with the exception of articular cartilage removed.
- Registration block and wires attached to the iliac crest to reproduce the boundary conditions in the FE model.
- Volumetric CT scan (512 x 512 acq. matrix, FOV = 225 mm, 354 slices, slice thickness = 0.6 mm).
- Iliac crests submerged in a mounting pan of catalyzed polymer resin to a depth defined by the iliac guide wires.
- Ten rosette strain gauges attached throughout the left hemipelvis (Fig. 1).
- 3D coordinates of the strain gauges and registration block determined using an electromagnetic digitizer.
- Vertical loads (0.25, 0.50, 0.75, and 1.0 X BW) applied to the acetabulum via a femoral prosthesis, attached to a linear actuator (Fig. 2).

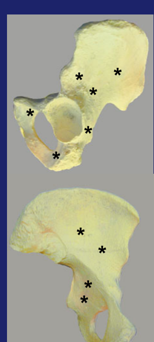

FIGURE 1 : Model indicating the 10 locations of rosette strain gauges used on the cadaveric pelvis.

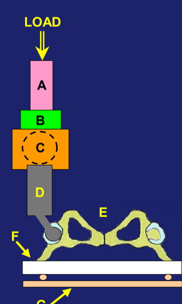

FIGURE 2 : Fixture for loading the pelvis (A) actuator, (B) load cell, (C) ball joint, (D) femoral component, (E) pelvis, (F) mounting pan for embedding pelvis, and (G) lockable X-Y translation table.

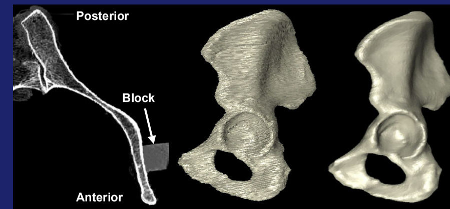

FIGURE 3 : Left - CT image slice at the ilium, showing the registration block. Middle - the original reconstructed surface. Right - surface after decimation to reduce the number of polygons and smoothing to reduce high-frequency digitizing artifact.

FE Model Generation -

- Separate surfaces for outer cortex and boundary of cortical and trabecular bone extracted from CT data (Fig. 3).
- FE model created from the surfaces, consisting of triangular shell elements for cortical bone and tetrahedral solid elements for trabecular bone (Fig. 4).
- Acetabular cartilage represented with shell elements at constant thickness of 2 mm.
- Novel algorithm developed to assign a spatially varying cortical shell thickness.

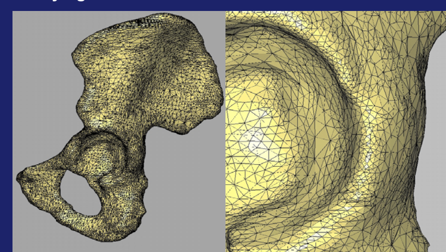

FIGURE 4 : FE mesh of the pelvis (left) with a close-up view of the mesh at the acetabulum (right).

FE Boundary Conditions / Analysis -

- Cortical bone E = 17 GPa and ν = 0.29 [1].
- Relationships between CT Hounsfield unit, apparent density and elastic modulus used to assign a density-dependent modulus for each tetrahedral element [2,3], with ν = 0.21 [1].
- Acetabular articular cartilage represented as a hyperelastic Mooney-Rivlin material [4].
- Nodes superior to the cement line and those along the pubis joint defined as rigid.
- LS-DYNA used for all analyses; FE predictions of maximum and minimum cortical principal strains averaged over elements that were located beneath strain gauges.

Sensitivity Studies -

- Variations in assumed and measured parameters were assessed.
- *Assumed Parameters*: cortical and trabecular bone ν, cartilage thickness & modulus, cortical bone elastic modulus.

RESULTS

The algorithm predicted cortical bone thickness between 0.4 - 3.0 mm (mean 1.0 ± 0.4 mm) (Fig. 5). The subject-specific FE model predictions of principal strains corresponded very well with experimental measures (Fig. 6, top right).

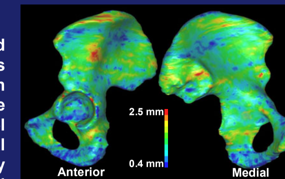

FIGURE 5 : Contours of position dependent cortical thickness.

Models representing standard deviations in average trabecular elastic modulus did not alter strains considerably (Fig. 6, bottom left). In contrast, changes to cortical bone thickness had a substantial effect on cortical bone strains (Fig. 6, bottom right). Alterations to all other parameters did not have a significant effect (data not shown).

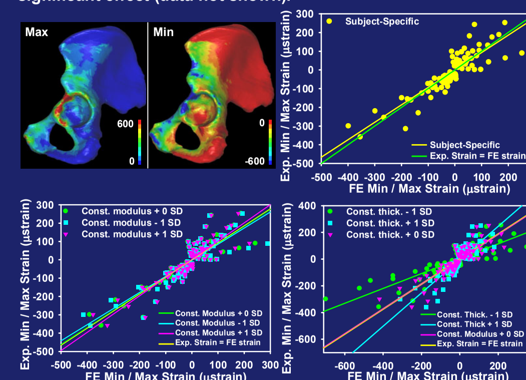

FIGURE 6 : Top left - contours of subject-specific max / min principal strain (μstrain). FE predicted vs. experimental cortical bone principal strain; Top right - subject-specific strains. Bottom left - constant trabecular modulus. Bottom right - constant cortical thickness.

DISCUSSION

This research demonstrated that a subject-specific FE model of the pelvis was able to predict experimentally measured cortical bone strains. The model with an average thickness produced accurate results; however, the thickness of the cortex beneath the gauges was very close to the model average but deviated much less. Thus, accurate measurement of thickness should still be considered. Although changes to trabecular bone modulus had only a slight effect on cortical strains, overall model displacement was significantly altered, which suggests that the trabecular bone should be included.

In contrast to previous FE studies of the pelvis, detailed pelvic FE mesh geometry, incorporating a position dependent cortical bone thickness, was recreated from subject-specific CT image data. Further, by applying a well-defined experimental loading configuration, the applied loads were reproduced in the FE model with minimal error. The results of this study provide the basis for future efforts to analyze patient-specific FE models of the pelvis to elucidate the biomechanics of hip dysplasia and total hip reconstruction.

REFERENCES

[1] Dalstra M, et al., J Biomech Eng 117:272-78, 1995. [2] Dalstra M, et al., J Biomech 26:523-35, 1993. [3] Ploeg H, et al., NAFEMS World Congress 811-22, 2001. [4] Little R, et al., J Biomech Eng 34:111-19, 1986.